

Electronic Supplementary Information

**Graphene Nanoparticles Decorated Silicon Nanowires with Tungsten Oxide Counter
Electrode for Quasi Solid-State Hybrid Solar Cells**

Ankita Kolay,^a Manoranjan Ojha,^a Melepurath Deepa^{*,a}

^aDepartment of Chemistry, Indian Institute of Technology Hyderabad, Kandi, Sangareddy,
Telangana 502285, India.

E-mail: mdeepa@chy.iith.ac.in

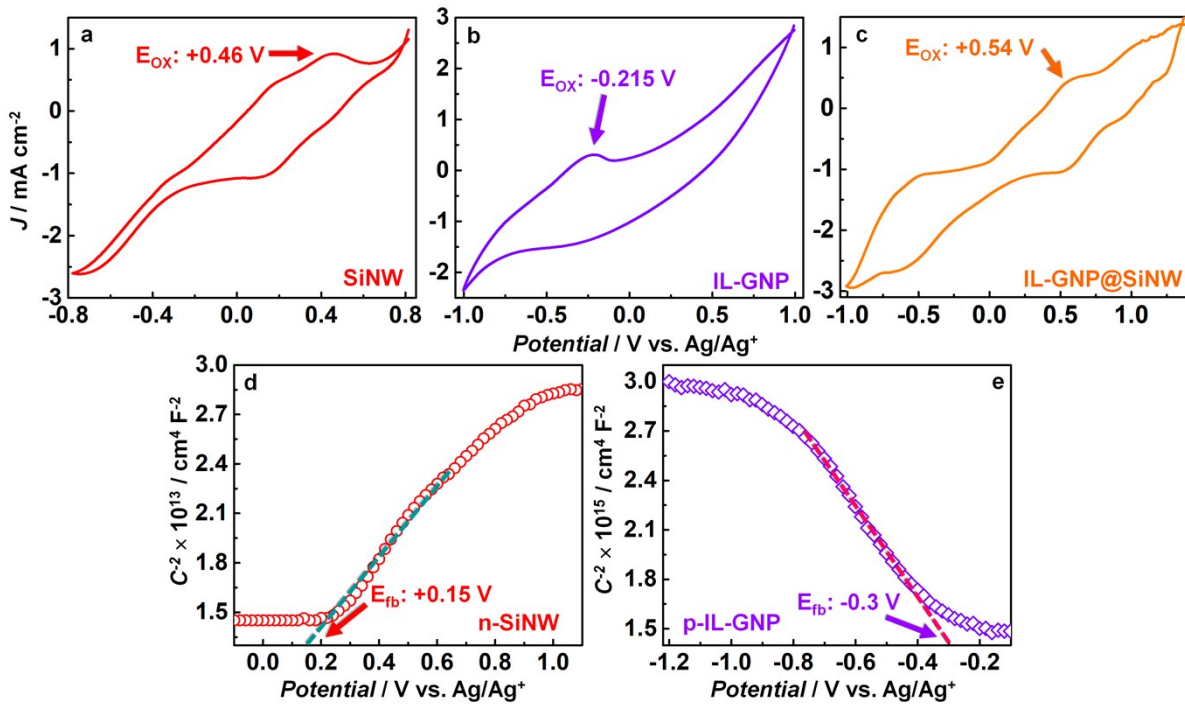


Figure S1 CV plots of (a) SiNW, (b) IL-GNP and (c) IL-GNP@SiNW in three electrode cells, with 0.1 M KCl as the electrolyte, a Pt rod as the counter electrode and Ag/AgCl/KCl as the reference. Mott-Schottky plots of (d) SiNW and (e) IL-GNP in the same cell configuration in dark. The intercepts are the flat band potentials in (d) and (e).

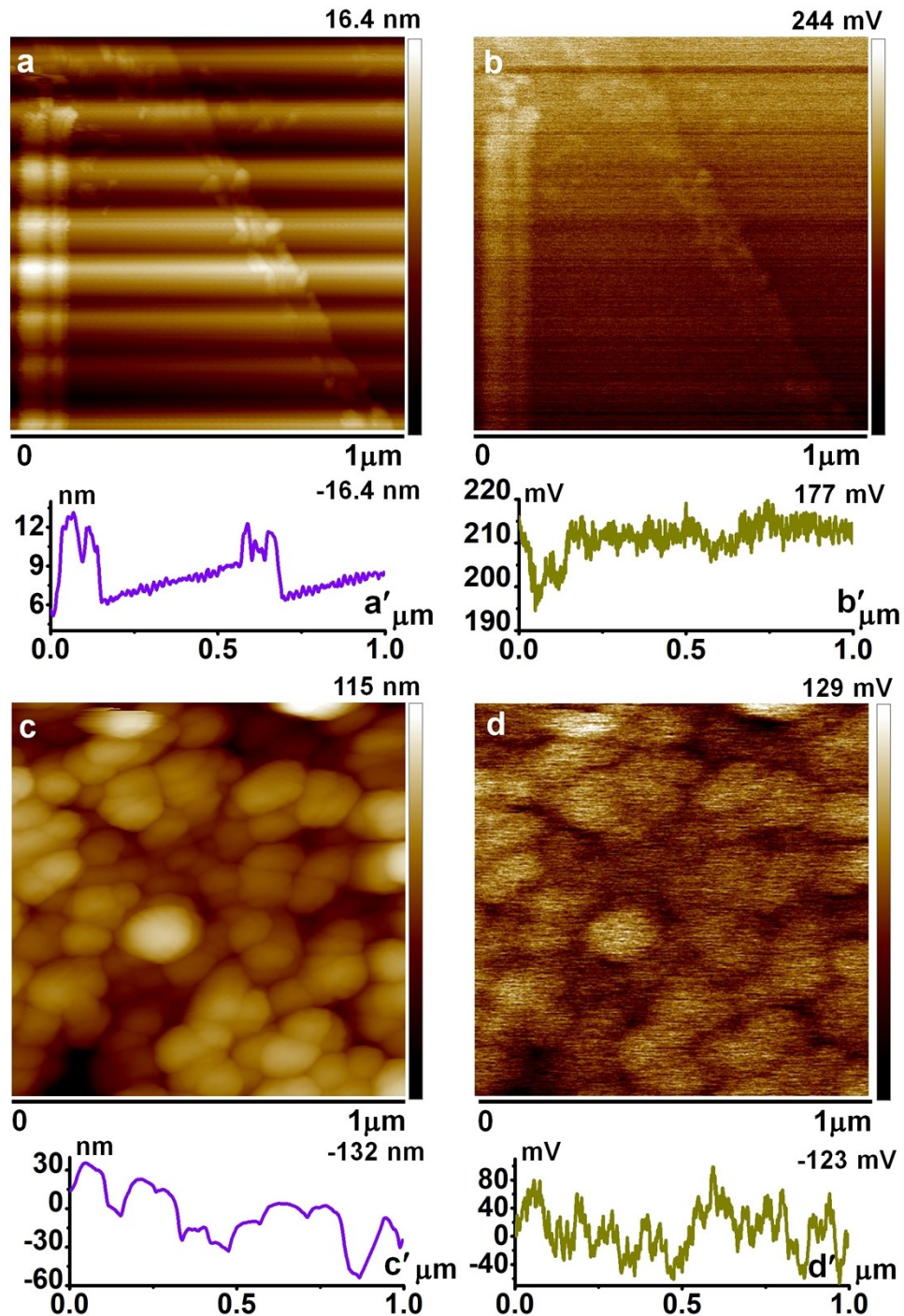


Figure S2 Topography (a,c) and surface potential maps (b,d) of HOPG and WO_3 , and the corresponding representative section profiles are shown in (a',c') and (b',d') respectively.

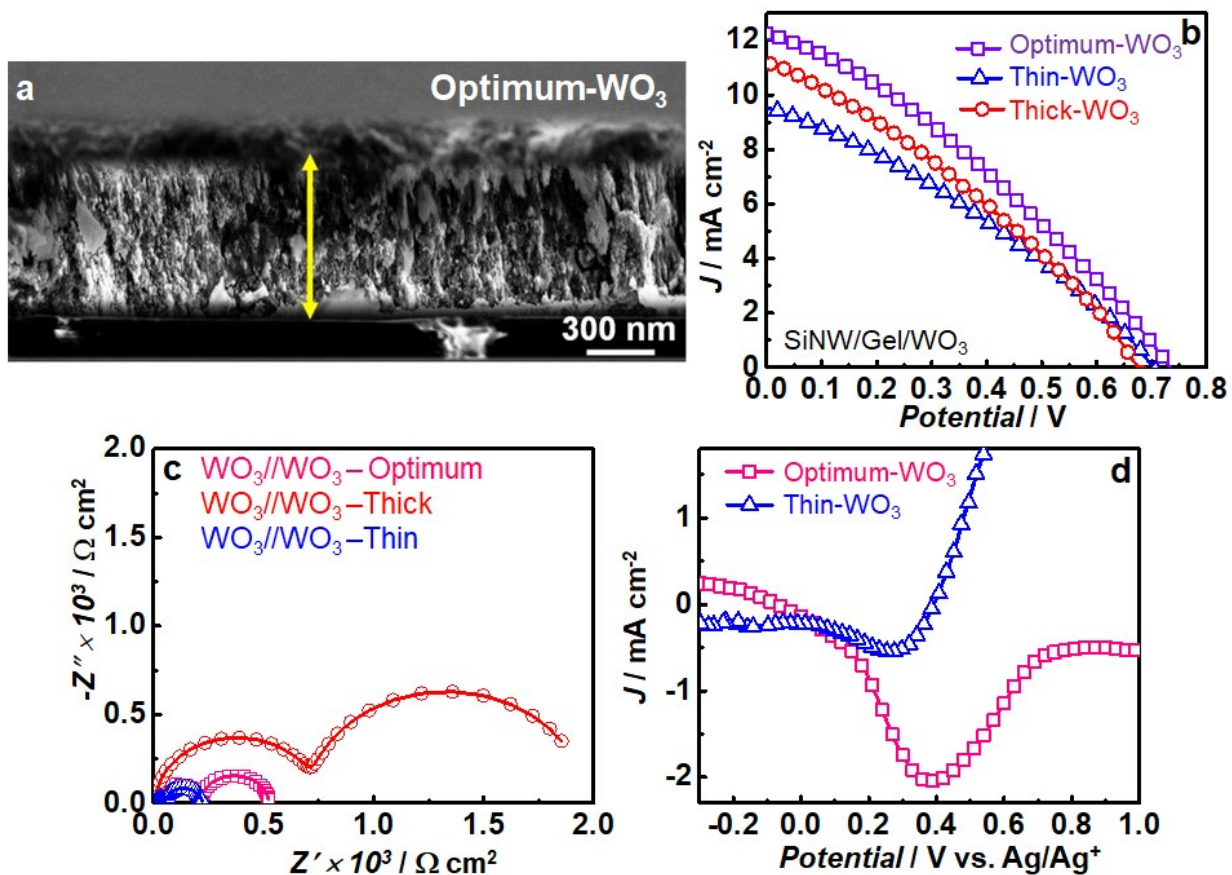


Figure S3 (a) Cross-sectional SEM image of a WO_3 @FTO film. (b) J-V characteristics of $\text{SiNW}/\text{gel}/\text{WO}_3$ cells, with varying WO_3 thicknesses, based on electrodeposition span. (c) Nyquist plots compared for symmetric cells of WO_3 (of different thicknesses) with $\text{BMIM}^+\text{I}^-/\text{I}_2$ gel over 10 mHz to 1 MHz. (d) I-V plots comparing the tri-iodide reduction capability of WO_3 films of different thicknesses, with Pt as the counter electrode.

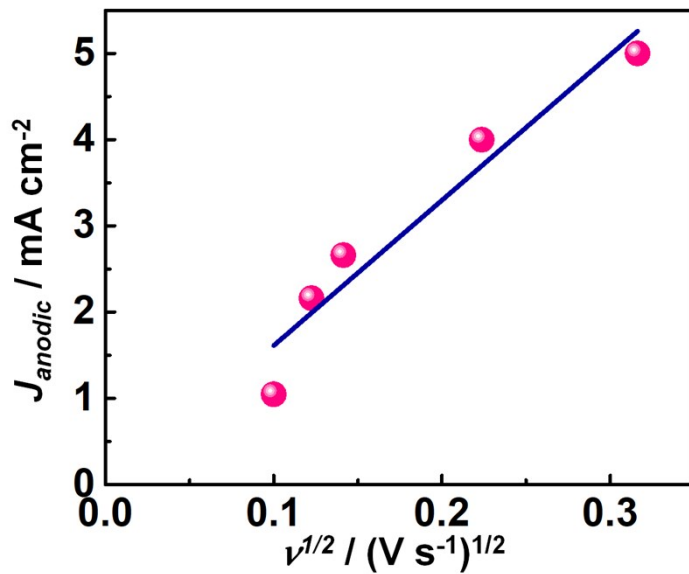


Figure S4 Linear dependence of anodic peak current density versus square root of scan rate for a WO_3 film.

Table S1 Fitted parameters for Nyquist plots for symmetric cells based on the gel electrolyte composed of 1 M BMIM⁺I⁻, 0.05 M I₂, 2 wt% poly(AMPS) and 7 wt% SiO₂ in PC.

| Cell | R_1 (R_{gel} , Ω cm^2) | R_2 (R_{electron} , Ω cm^2) | R_3 (R_{ct} , $\Omega \text{ cm}^2$) | C_2 (C_{μ} , F cm^2) | C_3 (C_{dl} , F cm^2) |
|---|---|--|--|--|--|
| FTO// WO_3 // WO_3 /FTO | 6.3 | 206.2 | 312.5 | 1.2×10^{-5} | 3.4×10^{-3} |
| FTO//FTO | 10.6 | 33.2 | 4286 | 3.6×10^{-5} | 2×10^{-3} |

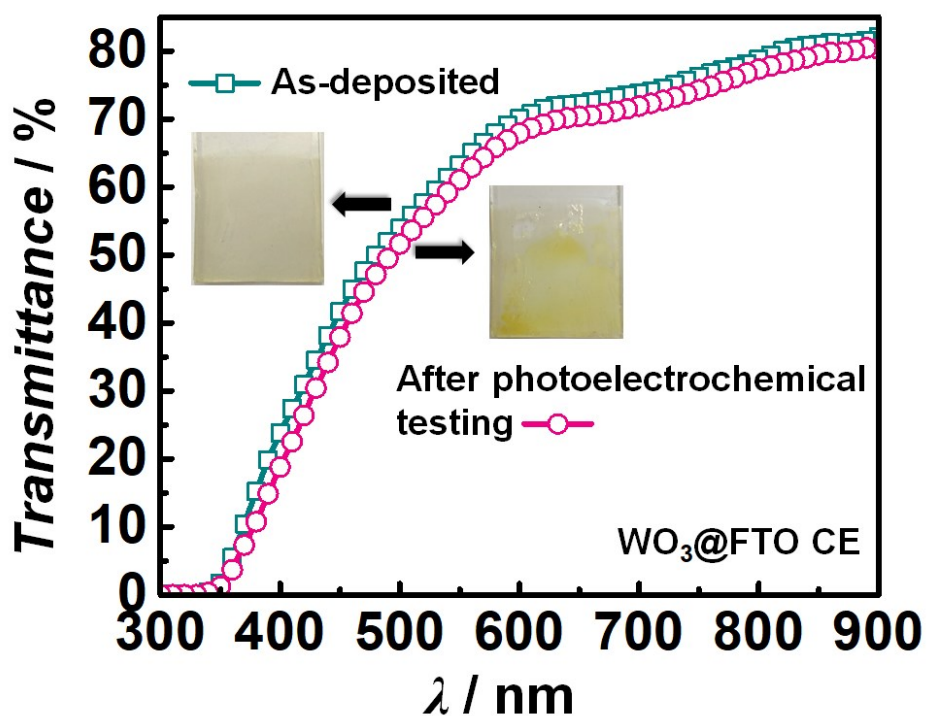


Figure S5 Transmittance spectra of a WO_3 CE film before and after the solar cell stability test.

Table S2 Solar cell parameters for different cells, standard deviation on 5-cell data.

| Cells | V _{OC} (mV) | J _{SC} (mA cm ⁻²) | FF | PCE (%) |
|------------------------------------|----------------------|--|-------------|-----------|
| SiNW/Gel/WO ₃ | | | | |
| Cell 1 | 754 | 13.62 | 0.461 | 4.73 |
| Cell 2 | 644 | 12.19 | 0.427 | 3.35 |
| Cell 3 | 674 | 12.37 | 0.436 | 3.64 |
| Cell 4 | 704 | 12.91 | 0.445 | 4.05 |
| Cell 5 | 724 | 13.19 | 0.451 | 4.31 |
| Average | 700±43 | 12.86±0.59 | 0.444±0.013 | 4.02±0.54 |
| SiNW/Liquid/WO ₃ | | | | |
| Cell 1 | 731 | 12.22 | 0.316 | 2.83 |
| Cell 2 | 631 | 10.60 | 0.296 | 1.98 |
| Cell 3 | 661 | 11.02 | 0.301 | 2.19 |
| Cell 4 | 691 | 11.42 | 0.308 | 2.43 |
| Cell 5 | 701 | 11.70 | 0.310 | 2.54 |
| Average | 683±38 | 11.39±0.62 | 0.306±0.008 | 2.39±0.33 |
| IL-GNP@SiNW/Gel/WO ₃ | | | | |
| Cell 1 | 768 | 18.39 | 0.562 | 7.93 |
| Cell 2 | 753 | 17.32 | 0.558 | 7.28 |
| Cell 3 | 740 | 17.92 | 0.557 | 7.38 |
| Cell 4 | 738 | 17.25 | 0.556 | 7.08 |
| Cell 5 | 718 | 16.75 | 0.551 | 6.63 |
| Average | 743±19 | 17.53±0.64 | 0.557±0.004 | 7.26±0.47 |
| IL-GNP@SiNW/Liquid/WO ₃ | | | | |
| Cell 1 | 761 | 17.23 | 0.487 | 6.39 |
| Cell 2 | 683 | 15.83 | 0.462 | 5.00 |
| Cell 3 | 673 | 15.39 | 0.459 | 4.76 |
| Cell 4 | 733 | 16.36 | 0.477 | 5.72 |
| Cell 5 | 703 | 16.16 | 0.468 | 5.32 |
| Average | 711±36 | 16.19±0.69 | 0.471±0.011 | 5.44±0.64 |

Table S3 Comparison of n-SiNW based solar cells from photovoltaic literature.

| Solar Cell Architecture | J_{SC} (mA cm ⁻²) | V_{OC} (mV) | FF | PCE or η (%) | Reference |
|--|------------------------------------|------------------|-----------------|----------------------|-----------|
| Al/p-Si-n-SiNW/TCO/polymer (0.6 cm ²) | 2 | 230-280 | 0.2 | 0.1 | 1 |
| Glass/mc-p-Si/mc-n-SiNW/mc-n ⁺ -SiNW/Au (0.64 mm ²) | 40 | 450 | - | 4.4 | 2 |
| PIN-RJSiNW | 14.6 | 750 | 0.581 | 6.32 | 3 |
| n-SiNW/p-SiNW/Al/Pd (8 μm absorber) | 16.82 ± 0.50 | 525 ± 2 | 0.559 ± 0.02 | 5.30 ± 0.19 | 4 |
| p-i-n -coaxial SiNW (upper bound) | 23.9 ± 1.2 | 260 | 0.55 | 3.4 ± 0.2 | 5 |
| p-i-n -coaxial SiNW (lower bound) | 16 ± 0.8 | 260 | 0.55 | 2.3 ± 0.2 | 5 |
| ITO/V ₂ O ₅ /n-SiNW/TiO ₂ /Al | 35.7 | 490 | 0.727 | 12.7 | 6 |
| ITO/n-SiNW/TiO ₂ /Al | 20.4 | 214 | 0.425 | 1.86 | 6 |
| AZO core–shell TCO/a-Si/n-SiNW (7 mm ²) | 27 | 476 | 0.562 | 7.29 | 7 |
| Al/n-SiNW/PEDOT/ITO | 19.28 | 470 | 0.61 | 5.09 | 8 |
| Al/n-SiNW/Spiro-OMeTAD/PEDOT:PSS/Ag | 26.7 | 530 | 0.643 | 9.2 | 9 |
| Al/n-SiNW-DADS/PEDOT:PSS/Ag | 28.80 ± 1.03 | 488 ± 6 | 0.49 ± 0.012 | 7.02 ± 0.17 | 10 |
| n-SiNW/40%HBr, 3%Br ₂ /Pt mesh | 0.872 | 730 ± 20 | 0.45 | 0.286 | 11 |
| PtNPs/C@n-SiNW/8.6M HBr, 0.05Br ₂ /Pt mesh | 36.89 | 530 | 0.555 | 10.86 | 12 |
| n-SiNW-CH ₃ (Pt)/0.05 M I ₂ , 0.1 M LiI in a mixed IL (EMISCN:PMII, 7:13, v/v)/Pt - ITO | 33.7 | 322 | 0.40 | 4.3 | 13 |
| n-SiNW-PtNPs/8.6M HBr, 0.05Br ₂ /Pt | 24.26 | 550 | 0.61 | 8.14 | 14 |
| n-SiNW-AuNPs/8.6M HBr, 0.05Br ₂ /Pt | 14 | 745.3 | 0.23 | 2.4 | 14 |
| Se NPs@Si NWs/8.6M HBr, 0.05Br ₂ /C-fabric | 17.12 | 790 | 0.52 | 7.03 | 15 |
| C@TeNRs@Si NWs/8.6M HBr, 0.05Br ₂ /C-fabric | 23.27 | 893 | 0.56 | 11.59 | 16 |
| IL-GNP@SiNW/I ₂ ,I ⁻ gel/WO ₃ | 18.39 | 768 | 0.56 | 7.93 | This work |

TCO: Transparent conducting coating, mc: Multicrystalline, RJ: Radial junction, AZO: Al doped ZnO, a: Amorphous, Spiro-OMeTAD: 2,2',7,7'-Tetrakis-(N,N-di-4-methoxyphenylamino)-9,9'-spirobifluorene, ITO: In₂O₃:Sn coated glass, PEDOT: Poly(3,4-ethylenedioxothiophene), PSS: Poly(4-styrenesulfonate), DADS: Diallyl disulfide, IL: Ionic liquid, PMII: 1-Propyl-3-

methylimidazolium iodide, EMISCN: 1-Ethyl-3-methylimidazolium thiocyanate, NPs: Nanoparticles, IL-GNP: Ionic liquid functionalized graphene nanoparticles.

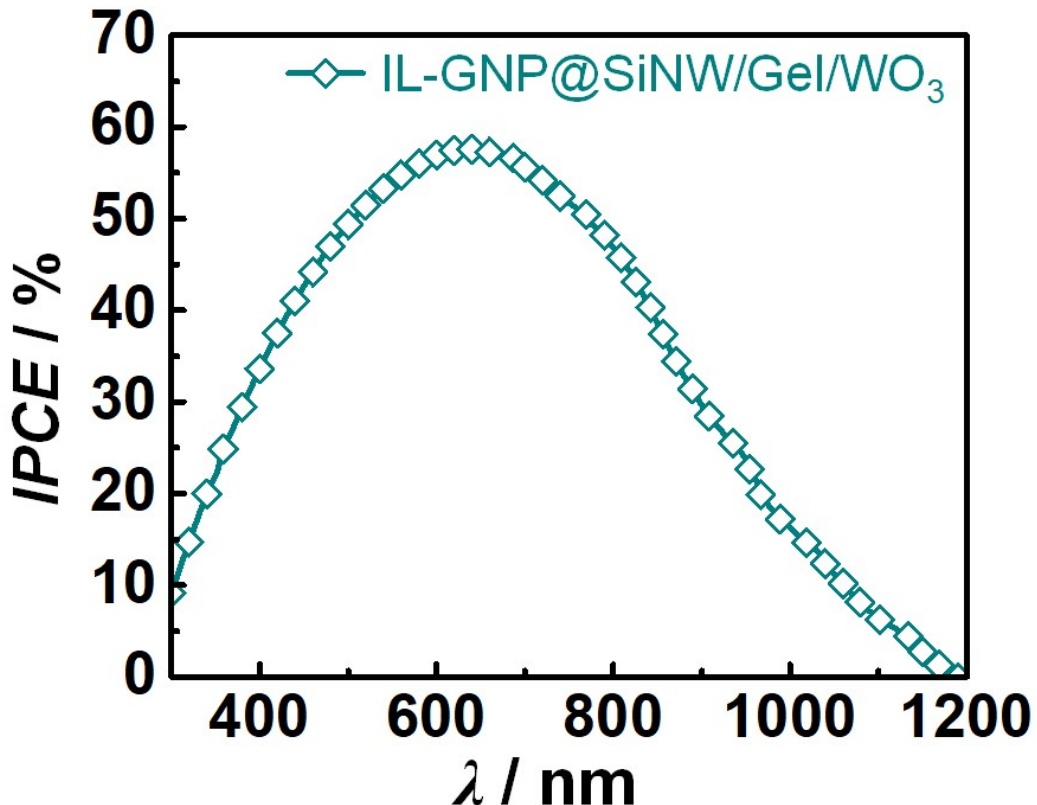


Figure S6 IPCE plot for the IL-GNP@SiNW/Gel/WO₃ hybrid solar cell.

References

1. T. Stelzner, M. Pietsch, G. Andra, F. Falk, E. Ose and S. Christiansen, *Nanotechnology*, 2008, **19**, 295203.
2. V. Sivakov, G. Andra, A. Gawlik, A. Berger, J. Plentz, F. Falk and S. H. Christiansen, *Nano Lett.*, 2009, **9**, 1549–1554.
3. M. Al-Ghzaiwat, M. Foldyna, T. Fuyuki, W. Chen, E. V. Johnson, J. Meot and P. Roca i Cabarrocas, *Sci Rep*, 2018, **8**, 1651
4. E. Garnett and P. Yang, *Nano Lett.*, 2010, **10**, 1082–1087

5. B. Tian, X. Zheng, T. J. Kempa, Y. Fang, N. Yu, G. Yu, J. Huang and C. M. Lieber, *Nature*, 2007, **449**, 885–890.
6. G. Ma, R. Du, Y. n. Cai, C. Shen, X. Gao, Y. Zhang, F. Liu, W. Shi, W. Du and Y. Zhang, *Sol Energy Mater Sol Cells*, 2019, **193**, 163–168.
7. G. Jia, M. Steglich, I. Sill and F. Falk, *Sol. Energy Mater. Sol. Cells*, 2012, **96**, 226–230.
8. S. C. Shiu, J. J. Chao, S. C. Hung, C. L. Yeh and C. F. Lin, *Chem. Mater.*, 2010, **22**, 3108–3113.
9. L. He, C. Jiang, H. Wang, D. Lai and Rusli, *ACS Appl. Mater. Interfaces*, 2012, **4**, 1704–1708.
10. Y. Rui, T. Zhang, D. Zhu, Y. Feng, A. N. Cartwright, M. T. Swihart, Y. Yang, T. Zhang, C. Huang, H. Wang and D. Gu, *J. Phys. Chem. C*, 2019, **123**, 4664–4673.
11. K. Peng, X. Wang and S. T. Lee, *Appl. Phys. Lett.*, 2008, **92**, 163103.
12. X. Wang, K. Q. Peng, X. J. Pan, X. Chen, Y. Yang, L. Li, X. M. Meng, W. J. Zhang and S. T. Lee, *Angew. Chem. Int. Ed.*, 2011, **50**, 9861–9865.
13. X. Shen, B. Sun, F. Yan, J. Zhao, F. Zhang, S. Wang, X. Zhu and S. Lee, *ACS Nano*, 2010, **4**, 5869–5876.
14. K. Q. Peng, X. Wang, X. L. Wu and S. T. Lee, *Nano Lett.*, 2009, **9**, 3704–3709.
15. A. Kolay, D. Maity, P. Ghosal and M. Deepa, *J. Phys. Chem. C*, 2019, **14**, 8614–8622.
16. A. Kolay, D. Maity, P. Ghosal and M. Deepa, *ACS Appl. Mater. Interfaces* 2019, **11**, 47972–47983.